Check for updates

Journal of Climate Change, Vol. 7, No. 3 (2021), pp. 23-33.
DOI 10.3233/JCC210016

Seasonal Characteristics of Temperature Gradient in a Glaciated Catchment in Eastern Himalaya

Pradeep Vashisht[1] and Shresth Tayal[2]*

[1]TERI School of Advanced Studies, New Delhi - 110 070, India
[2]The Energy and Resources Institute (TERI), New Delhi - 110 003, India
✉ Stayal.glaciers@gmail.com

Received March 18, 2020; revised and accepted June 28, 2021

Abstract: With climatic information from four stations in Rathong Chu valley for the period from 2017 to 2018, this study presents monthly and seasonal characteristics of the temperature lapse rate (TLR) in the eastern Himalayas. The station heights utilised in the study ranged from 1,742 to 4,450 m. The TLRs were assessed utilising a linear regression model. The mean yearly TLR for eastern Himalaya is less sheer (−0.52°C/100 m) beneath the tree line than (−0.47°C/100 m) over the tree line. The series of TLR exhibits two peaks in a year which confirms the distinctive controlling elements in the individual seasons. The highest TLR was found to be −0.60 °C/100 m during the pre-monsoon season below the tree line and −0.64 °C/100 m above the tree line. The post-monsoon has the second highest lapse rate change beneath the tree line (−0.58 °C/100 m) and in the monsoon (−0.57 °C/100 m) above the tree line. The minimum lapse rates were observed in the winter season below the treeline (−0.42 °C/100 m) and (−0.18 °C/100 m) above the tree line. The outcomes of this study add to the insight of elevation-dependent warming affected by worldwide climate change. Results also suggest that the climate and glacier modelling using the satellite temperature records or by applying the environmental lapse rate on temperature records from low altitudes may not be presenting the actual temperature trends.

Keywords: Temperature lapse rate; Monthly variation; Eastern Himalayas; Subtropical forest and Alpine meadows.

Introduction

The air temperature decreases with increasing elevation which is commonly known as temperature lapse rate (TLR) (Kattel et al., 2013). A rise in temperature has been shown by climate models using near-surface records of temperature (IPCC, 2013). In mountainous regions around the globe various studies suggest that there is an increased rate of warming, particularly in the minimum temperatures as compared to the nearby low land areas (Rangwala and Miller, 2012). The rising temperature has a negative impact on the glacio-hydrology of snow/ice-fed river catchments (Barnett et al., 2005). TLR is one of the most substantial traits of regional climates (Micu et al., 2015). Studies conducted on TLR changes indicate that the temperature varies with height due to the background air mass lapse rate (Kattel et al., 2013; Heynen et al., 2016; Hanna et al., 2017; Kattel et al., 2018; Kattel et al., 2019; Yadav et al., 2019) and it gets further depressed in valleys due to the formation of cold air pools (Bogren et al., 2000). The Himalayan glaciers due to their topographical settings are vulnerable to the slightest changes in temperature and patterns of precipitation (Immerzeel et al., 2010). Studies have accentuated the significance of the ambient air TLR in estimating temperature values at higher altitudes (Blandford et al., 2008; Gardner et al., 2009; Kattel et al., 2013, 2015; Kattel et al., 2018;

*Corresponding Author

Romshoo et al., 2018; Thayyen and Dimri, 2018; Joshi et al., 2018; Kattel et al., 2019).

The temperatures in the Himalayas are controlled by a complex system driven by topography, seasons, and cryosphere which hindrances the in situ air temperature observations (Singh et al., 2019). Ambient air temperature is an important proxy for energy exchange between land surface and atmosphere, hence it becomes a pivotal parameter in climate research (Jones et al., 1994; Hansen et al., 2010; Singh et al., 2019). The surface and near-surface air temperature records are key to glacio-hydro-climatological studies further if extrapolated to different elevations using a calculated lapse rate can provide more realistic estimates. Lapse rates of temperature may shift with latitude, topographic slant, locales, and season (Dodson and Marks, 1997; Bolstad et al., 1998; Rolland, 2003; Immerzeel et al., 2014) and hence can't be treated as spatially and transiently steady. In the Himalayan landscape, the atmospheric conditions at the regional and local scales are influenced by geography, latitude, movement of air masses, and types of flora (Barry, 1992). Due to these variables, temperature and precipitation in this locale changes strikingly even over a short geographic separation and henceforth the regional circulation of temperature and precipitation fluctuate along altitudinal inclination. Fundamentally, the estimations of temperature made for the local level based on the general temperature-elevation patterns may not represent reality adequately.

There are two main approaches to model melt from a glacierised catchment namely energy balance approach and temperature index or degree-day approach (Hock, 2003). Due to computational simplicity and fewer input parameters, the degree-day approach has been widely used in mountainous catchments (Hock, 2003) because it does not require several weather parameters like net radiation, relative humidity and wind speed and direction (Azam et al., 2014). Air temperature is a good index for snow and ice melt estimation as it can be used as a proxy for the components of energy balance models (Ohmura, 2001). The temperature lapse rate can be used for temperature extrapolation to the higher altitude which could improve the efficiency of climate and hydrological models by better representation of the climate along the Himalayan slopes. The near surface TLR is a controlling element of numerous natural processes. Subsequently, the altitudinal reliance of temperature in mountain areas is essential to study the effects of climate change on different processes such as atmosphere vegetation interactions, snow cover area, and glacier melt variations and corresponding melt runoff, change in hydrological cycles, etc. Hanna et al. (2017) stated that a temperature lapse rate of 30 minutes or lesser time interval is more accurate to feed into the glacier and snowmelt models. A few investigations have affirmed that the temperature lapse rate is an important factor in reality in mountain areas and its magnitude may vary at various locations as a function of energy balance (Gardner et al., 2009; Kattel and Yao, 2013; Thayyen and Dimri, 2014; Kattel et al., 2018). The investigations of the mountainous regions which envelope wide climatic elevational inclinations in the Himalayas are restricted, due to absence of meteorological information. The eastern Himalayan uplands inhabit unique and important ecological habitats and supply water to various perennial rivers. The instrumental climatic records in these uplands ensure their use in understanding climate change. In this regard, a study conducted by Agrawal and Tayal (2015) examined the temperature lapse rates using the gridded data (IMD data and APHRODITE data) and their controlling elements in the eastern Himalayas in Sikkim.

The present study is an attempt to analyse the temperature records for the high-altitude valley in the eastern Himalayas to calculate and inspect monthly and seasonal variations in temperature lapse rate with changing altitude in the valley. We have installed temperature sensors to measure temperature in East Rathong Chu valley during 2017-2018 to compute the temperature lapse rate for the Valley. This study also examines the construction of temperature series for the higher altitude by implying the calculated temperature lapse rate and compare the accuracy of calculated TLR and Environmental lapse rate. The calculated TLR improves the efficiency of hydrological models to simulate ice/snowmelt runoff in the higher altitudes of the eastern Himalayas. Our results demonstrated the statistically strong spatial and seasonal representation of the constructed temperature series using the calculated TLR in the eastern Himalaya. We anticipate that our results will provide the scientists in Himalaya or similar data-deficient extreme environments with an option to use this calculated TLR in their models for more realistic estimates and to fill-up the spatiotemporal data gaps related to in situ monitoring.

Study Area

The Teesta River is a right-bank tributary of the Brahmaputra river, located in the eastern Himalayas.

Right-bank tributaries drain heavily glaciated areas with large snow-fields. Teesta is supplied with enormous volume of water from melting snow and ice, underground waters and very high rainfall. Rathong Chu is a major tributary to Rangeet river which provides enormous water supply to Teesta river. Upper Rangeet sub-basin has been selected as study area in present study. Monsoon climtes supports the evergreen rainforents in the sub basin that has a steep gradient. Southwest monsoon season superintends more than 80% of the total annual rainfall in these mountainous areas. Almost the entire Teesta basin receives majority of rainfall in monsoon season which is crucial for controlling the water balance in the region (Singh and Goyal, 2016).

Snow and glaciers cover the upper transect of this sub-basin of the Teesta river. The study area as shown in Figure 1 extends from 27° 37' 26.91" N, 88° 2' 30.94" E to 27° 20' 15.91" N, 88° 14' 53.94" E and lies in Khangchendzonga biosphere reserve. The elevation of the study area ranges between 1750 masl and 4450 masl and is characterized by Alpine, mixed temperate and deciduous to subtropical forests (Chhetri et al., 2013). Based on field observations, we consider the treeline to be lying around 4,000 masl (shown in Figure 1) in the valley, with dense forests located below this altitude and the valley being vegetated.

Materials and Methods

Meteorological Setup and Data Collection

Two sets of sensors were considered to estimate the TLR and its spatial variations over the study area. Two portable Onset's Tidbit v2 Temp Loggers were installed below the tree line and two Pluvio units were installed above the tree line i.e. elevation higher than 4000 m. The temperature loggers were shielded by PVC pipes to protect the Tidbit v2 from direct insolation so that the temperature records do not exaggerate. The Campbell Scientific temperature and humidity probe (HC2S3) was housed in an aspirated radiation shield. The edifice of the shield reflects the solar radiation but allows the air to pass through to probe the ambient temperature. All the sensors installed at different locations were programmed to record data at every 15 minutes interval, and the data

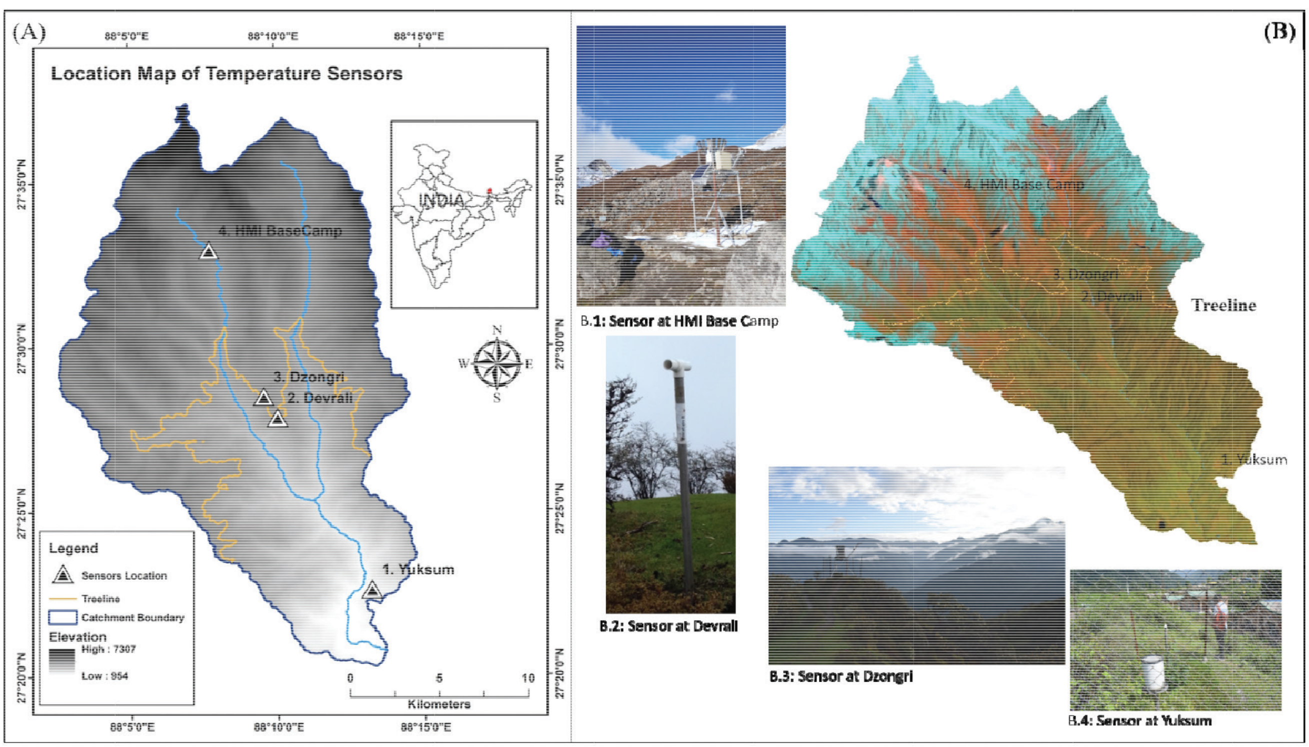

Figure 1: The map showing the location of the stations considered in the study for calculation of temperature lapse rate (TLR). (A) is showing the sensors location with elevation (Aster GDEM v2, 2011) profile of the region. (B) is showing the photographs of sensors used and the treeline (FCC created from Landsat 8 satellite image). B1 and B3 are the Pluvio Systems installed above the treeline and B2 and B4 are Tidbit V2 Temperature loggers installed below the treeline.

Table 1: Descriptions of the sensors used in the study

S. No.	*Site*	*Name of the sensor*	*Latitude/ Longitude*	*Altitude (masl)*	*Period of Record*	*Accuracy (°C)*
1	Yuksum	UTBI-001 Onset's Tidbit v2 Temperature Logger	88.2202 N 27.3777 E	1742 (Below treeline)	01 June 2017 to 31 May 2018	±0.2
2	Devrali	UTBI-001 Onset's Tidbit v2 Temperature Logger	88.1702 N 27.4646 E	3981 (Below treeline)		±0.2
3	Dzongri	Campbell temperature and humidity probe (HC2S3)	88.1592 N 27.4745 E	3965 (Above treeline)		±0.1
4	HMI BaseCamp	Campbell temperature and humidity probe (HC2S3)	88.1290 N 27.5494 E	4474 (Above treeline)		±0.1

from the stations were retrieved manually for the period of one year between June 2017 and May 2018.

The correlation coefficients between temperature and elevation of the weather stations were calculated for the observed dataset. Monthly mean, maximum, and minimum temperatures were correlated to elevations. Correlation analysis was carried out to estimate the strength of the linear relationship between temperature and elevation. The temperature lapse rates (in °C/100 m) were calculated by developing a regression equation using observations of temperature and elevation of all monitoring station locations. The developed regression determines the nature of the linear association between the two variables. TLRs were estimated using the following equation:

$$LR = \frac{T_1 - T_2}{z_1 - z_1} = \frac{dT}{dz} \quad (1)$$

where T_1 and T_2 are the respective air temperature of the highest and lowest points (in °C), and Z_1 and Z_2 are their respective elevations (in m). The temperature lapse rates were calculated using a regression model by scheming the strength of the correlation between temperature and elevation. Considering the fact that temperature in mountains is regulated by topography, aspect and seasonal patterns of climate (Barry, 1992), TLRs were calculated and analysed for the year and distinctly for the four main climatic seasons in the eastern Himalayas. Different seasons were recognised using the precipitation and temperature datasets from monitoring stations along with the literature reviewed (Kattel et al., 2013; Immerzeel et al., 2014) and were termed as monsoon (June-September), post-monsoon (October-November), winter (December-February) and pre-monsoon (March-May). XLSTAT software package was used to perform the statistical analyses of the obtained results.

Results

Correlation Between Elevation and Temperature

The air temperature has a linear relation with the elevation (Marshall and Sharp, 2009) under a well-mixed atmosphere (Lundquist, 2008). In this study, we found that the correlation between mean monthly temperature and elevation was significantly negative at $p < 0.05$ for all months. Among four seasons the lowest correlations were found during the winter season. The value of the correlation coefficient remained at the highest level in the pre-monsoon season. The temperature variations above and below the treeline environment witnessed a rise in temperature from mid-pre-monsoon to monsoon season but with different magnitudes. The relationship between the temperature and elevation is found to be robust with significant correlations ($R^2 = 0.98$ at $p < 0.05$), which paved the way to project temperature as a function of elevation.

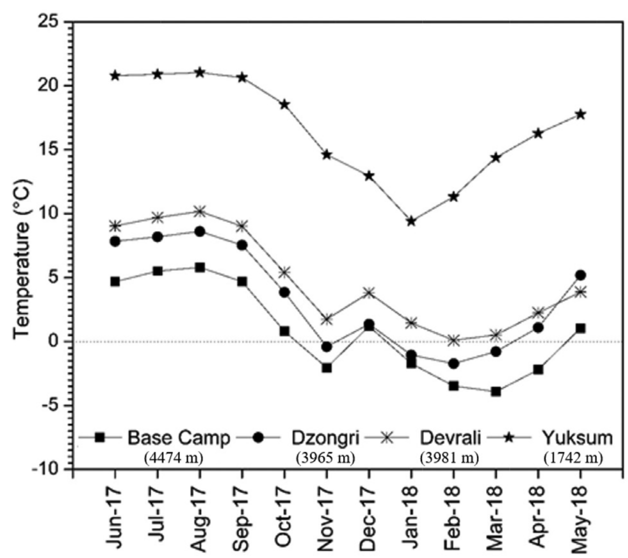

Figure 2: The mean monthly temperature of various monitoring stations used in the study.

Table 2: Monthly TLRs (in °C/100 m) below and above the treeline

	Monthly lapse rate: Below treeline			*Monthly lapse rate: Above treeline*		
Month	*Maximum TLR*	*Minimum TLR*	*Mean TLR*	*Maximum TLR*	*Minimum TLR*	*Mean TLR*
Jun-17	-0.55	-0.52	-0.53	-0.80	-0.51	-0.57
Jul-17	-0.53	-0.49	-0.50	-0.69	-0.55	-0.55
Aug-17	-0.48	-0.49	-0.48	-0.76	-0.59	-0.58
Sep-17	-0.58	-0.52	-0.52	-0.77	-0.56	-0.59
Oct-17	-0.62	-0.58	-0.59	-0.90	-0.63	-0.63
Nov-17	-0.62	-0.58	-0.57	-0.61	-0.50	-0.34
Dec-17	-0.46	-0.45	-0.41	-0.14	-0.11	-0.04
Jan-18	-0.32	-0.45	-0.36	-0.41	-0.26	-0.14
Feb-18	-0.42	-0.57	-0.50	-0.59	-0.48	-0.36
Mar-18	-0.65	-0.62	-0.62	-0.87	-0.67	-0.64
Apr-18	-0.68	-0.59	-0.63	-0.93	-0.83	-0.68
May-18	-0.60	-0.56	-0.56	-0.71	-0.63	-0.58

General Meteorological Characteristics

The observations of daily mean temperature and daily total precipitation at a high-altitude station (4450 masl) above treeline showed that approximately 85.3%, 2.4%, 0.7%, and 11.7% of the total annual rainfall occurred during monsoon, post-monsoon, winters and pre-monsoon season, respectively. Similarly, the recorded temperature also shows variation and is characterised by the lowest temperatures in the pre-monsoon season which increases progressively till the onset of monsoon (Figure 2). The monsoon season has received the highest amount of rainfall (1,756.4 mm) with an average temperature of 5.2 °C.

Monthly Variation in Temperature Lapse Rate

The monthly variation in lapse rates for the above and below treeline is shown in Figures 3 and 4. TLR values more negative than the seasonal mean are considered as a larger decrease in temperature with increasing elevation whereas the lesser negative values of TLR are considered as the temperature inversion (Kattel et al., 2013). Above the tree line, the mean, maximum and minimum TLR varied from −0.04 to -0.68 °C /100 m, -0.14 to - 0.93°C /100 m and −0.11 to −0.83 °C /100 m, respectively. While below the tree line, lapse rate for mean, maximum and minimum temperature varied from −0.36 to −0.63°C /100 m, −0.32 to −0.68°C/100 m and−0.45 to −0.62°C/100 m, respectively.

Seasonal and Annual variation in TLRs

The highest temperature lapse rate was observed during the pre-monsoon season period and the lowest during

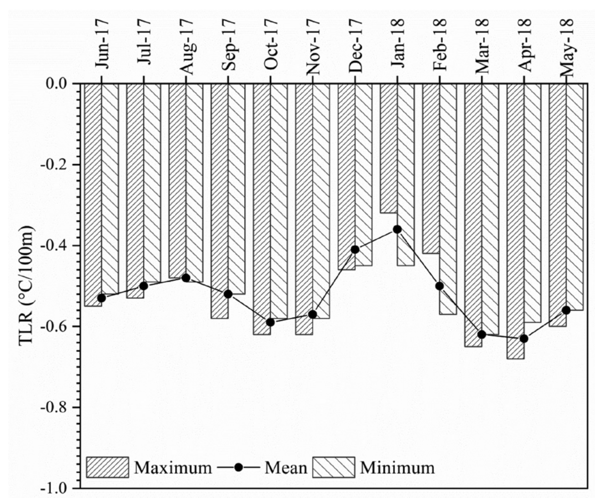

Figure 3: Variation in monthly TLRs above the treeline.

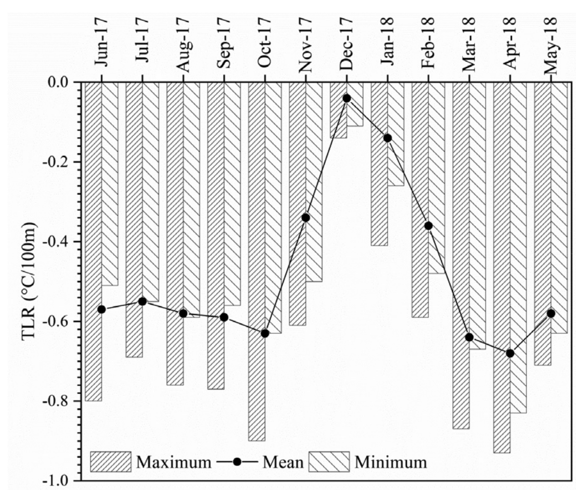

Figure 4: Variation in the monthly TLRs below the treeline.

Table 3: Seasonal TLRs (in °C/100 m) below and above the treeline

Season	*Seasonal lapse rate: Below treeline*			*Seasonal lapse rate: Above treeline*		
	Maximum TLR	*Minimum TLR*	*Mean TLR*	*Maximum TLR*	*Minimum TLR*	*Mean TLR*
Monsoon	-0.53	-0.50	-0.51	-0.75	-0.55	-0.57
Post-Monsoon	-0.62	-0.58	-0.58	-0.76	-0.57	-0.49
Winter	-0.40	-0.49	-0.42	-0.38	-0.28	-0.18
Pre-Monsoon	-0.64	-0.59	-0.60	-0.83	-0.71	-0.64

the winter season at both above and below the tree line environments, however, with different magnitude of lapse rates (Figures 6 and 7). The lapse rate for all the seasonal temperature parameters i.e., maximum, minimum and mean, was more variable in the above treeline environment as compared to the below treeline environment (Figure 5). The lack of vegetation above the tree line leads to a significant drop in temperature from hot to cold seasons and the lapse rate shows higher negative values in this region. Also, significant differences in the lapse rate between maximum and minimum temperatures were observed in all the seasons. On an annual scale, a higher value of mean TLR was observed below the treeline (−0.52°C/100 m) than above the treeline (−0.47°C/100 m). The analysis of the year-round cycle of lapse rate for maximum, mean and minimum temperature for above and below the treeline exhibits bimodal patterns with peaks in the pre-monsoon and post-monsoon seasons and two lowest values in the winter and monsoon seasons (Figures 6 and 7).

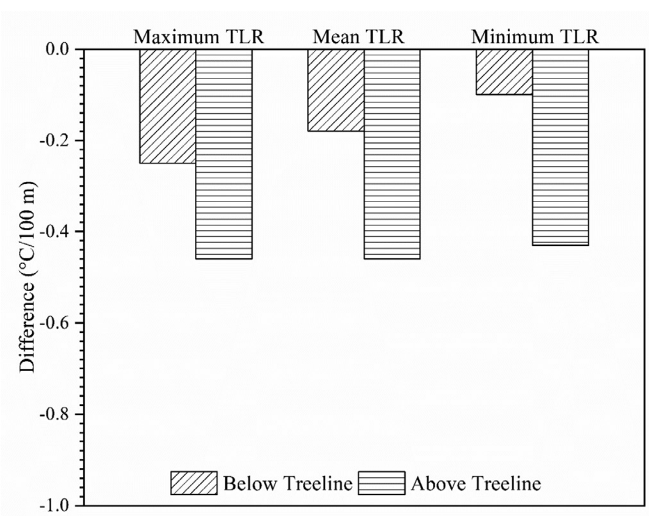

Figure 5: Difference between maximum and minimum across seasonal TLRs in below and above treeline environments.

Constructed Temperature using TLRs vs the Observed Temperature

To assess the applicability of calculated TLRs with reference to Environmental Lapse Rate (ELR), we

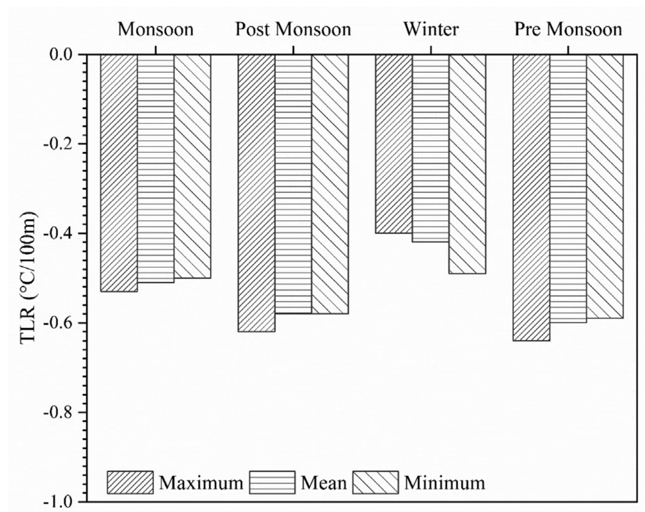

Figure 6: Seasonal variation in the TLRs below the treeline.

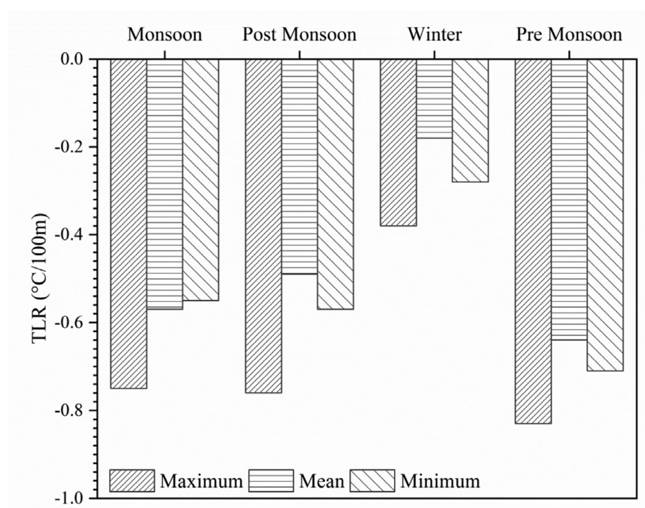

Figure 7: Seasonal variation in the TLRs above the treeline.

applied both the LRs to the temperature data available from the Indian Meteorological Department (IMD). IMD maintains a meteorological observatory at the Gangtok city (1650 masl) and long-term average temperature records of this station indicate a general cyclical pattern with a stable crest of high temperature from mid-May to September months (Figure 8).

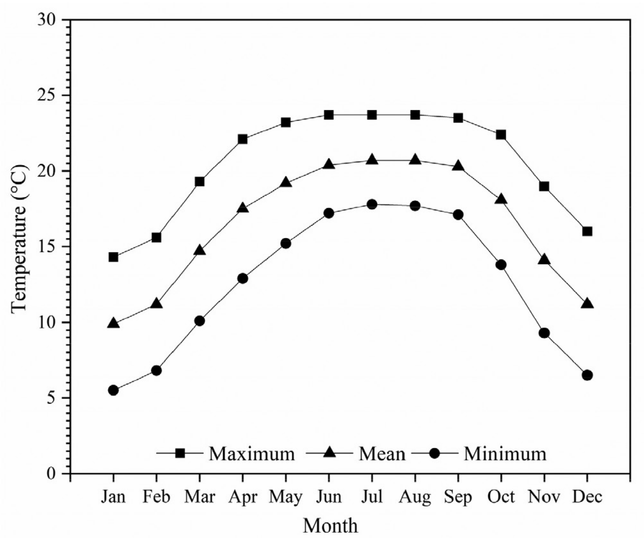

Figure 8: The mean monthly maximum temperature, mean monthly temperature, mean monthly minimum temperature of IMD Gangtok station (1,650 masl).

The constructed temperature series for monthly maximum, mean and minimum temperatures derived by applying TLR and ELR on Gangtok IMD data was compared with the station data observed at the HMI basecamp. The constructed temperature using the ELR (-0.65°C/100 m) and the observed temperature depicts that the ELR is not able to capture the monthly/seasonal variations in temperature at the higher altitude of the transect, whereas the series constructed using calculated monthly TLR has higher similarity to both trends as well as values of observed temperature at HMI basecamp (Figures 9-11).

Furthermore, we plotted the NASA POWER temperature data against the constructed as well as observed data for the HMI basecamp station, and similar results were obtained. The NASA Prediction of Worldwide Energy Resource (POWER) project provides distributed meteorological data that is easily available from the web site (power.larc.nasa.gov). Meteorological parameters are derived from NASA's GMAO MERRA-2 assimilation model and GEOS 5.12.4 FP-IT. MERRA-2 is a new version of NASA's Goddard Earth Observing System Data Assimilation

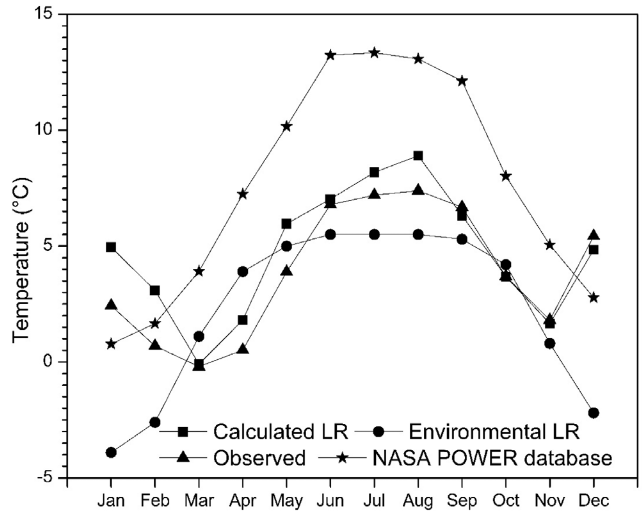

Figure 9: Comparison of average monthly maximum temperature at HMI Basecamp (4474 masl) constructed using calculated TLR, Environmental LR, modelled as well as observed.

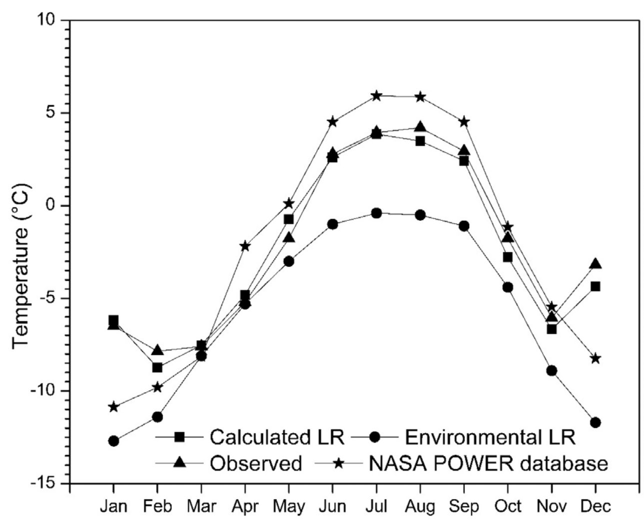

Figure 10: Comparison of average monthly minimum temperature at HMI Basecamp (4474 masl) constructed using calculated TLR, Environmental LR, modelled as well as observed.

System (GEOS). NASA POWER temperature is higher as compared to observed at the HMI Base Camp and does not capture the temperature variability pattern as observed data (Figures 9-11).

Discussion

The mean TLR values estimated using the data from weather stations along the elevational transect of the eastern Himalayas is lower than that of the environmental lapse rate (-0.65°C/100 m) and varies between elevation

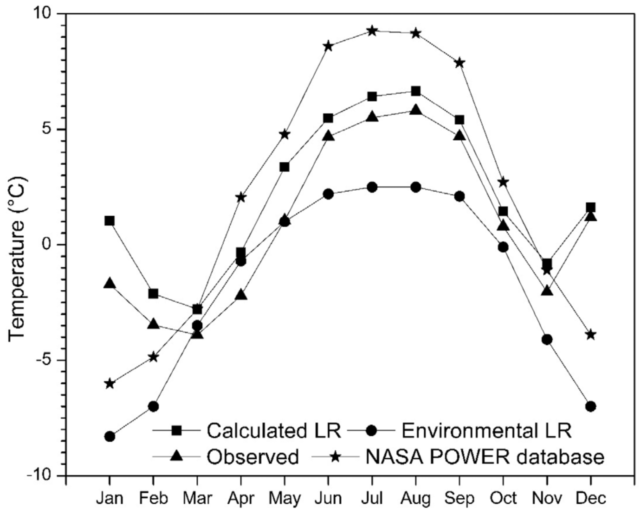

Figure 11: Comparison of average monthly temperature at HMI basecamp (4474 masl) constructed using calculated TLR, environmental LR, modelled as well as observed. Mean monthly temperature at HMI Basecamp (4474 masl).

covered with forests (−0.47°C/100 m below treeline) and elevation devoid of forests (−0.52°C/100 m above treeline). The lower lapse rate indicates that the thermal profile of higher elevation in the southern slopes of the Himalayas is warmer compared to general assumptions using the environmental lapse rate. These lower lapse rates may be expected due to the lower prevalence of free-air conditions and the release of longwave radiations from the mountain slopes. Furthermore, the variable lapse rates below and above the tree line are expected due to the prevalence of moist air under the influence of forests (Kattel et al., 2013). In addition, the cloud-free and comparatively drier atmosphere above the treeline is expected to increase the LR above the treeline (Immerzeel et al., 2014; Kattel et al., 2015).

This study also indicates that the lapse rate in the eastern Himalayas is not consistent throughout the year and shows a distinct bi-modal TLR pattern. The TLR peaks in the pre-monsoon and post-monsoon seasons and the two lowest values are recorded for the winter and monsoon seasons. This is due to the strong dominance of two synoptic weather systems influencing the regional climate. The Eastern Himalayan region experience a distinct summer wet season due to the monsoon system and also receives winter precipitation owing to westerlies. Again, the prevalence of moisture and cloud cover can be associated with temperature inversion effects that weaken the connection between temperature and altitude (Marshall et al. 2007), leading to the lowering of TLRs. The higher LRs for maximum temperature than that for minimum temperature on both sides of the tree line may be due to the adiabatic blending inside the boundary layer amid day time (Kattel et al., 2013).

Higher warming in the high altitude mountains is suggested by most of the climate models but with limited observations (Pepin and Lundquist, 2008). The solar radiation increases approximately 7-10%/km with height under cloud-free conditions (Barry, 1981). Due to the absence of clouds and higher temperatures in the pre-monsoon season, the earth’s surface gets greater incoming solar radiation relative to outgoing radiation. This phenomenon leads to a rise in daytime surface temperature and expansive sensible heat flux, which can improve solid dry convection within the daytime (Blandford et al., 2008). Moreover, the pre-monsoon season has the most noteworthy daytime saturation vapour pressure lapse rate (Kattel et al., 2013); as a result, TLR is highest in this season. The second highest TLR was noted amid the post-monsoon season except for mean temperatures above the treeline. The mean temperature lapse rate in this season was moderately lower as compared to the pre-monsoon season but higher in comparison to the winter and monsoon seasons.

The lowest TLR values were noted amid the winter season both over and underneath the tree line. The least TLR values in winter suggest that the other controlling variables play a more vital part. Clearer skies in the winter season lead to intense cooling by the outgoing longwave radiation at night times resulting in stable stratification and allow the formation of suitable microclimates for cold air deposition in the valleys (Thyer, 1985). The temperature inversion may be assisted by foggy conditions during the winter season (Rolland, 2003). The area covered by snow and resultant albedo in winters also impact the temperature lapse rate.

During the monsoon season, the second-lowest TLRs were noted when humidity in the atmosphere was high throughout the altitude spectrum because of the energy released by radiative relaxation during water vapour condensation. Temperature and humidity are the key factors influencing sensible and latent heat transfers (Marshall et al., 2007). Consequently, in response to rainfall during monsoon, the surface temperature decreases while humid adiabatic processes prevail (Thyer, 1985). In this way, the lapse rate for both maximum and minimum temperatures above and below the treeline suggests a firm affiliation with the amount of moisture present in the atmosphere, which is a specific feature to the eastern Himalayas in contrast to the western Himalayas having a predominance of winter precipitation. This demonstrates that the yearly cycle of vapour pressure plays a contributory role in improving and decreasing the TLRs amid dry (pre-monsoon season) and moist conditions (monsoon season), individually. Moreover, TLR variability is additionally administered by cloudiness. The thick cloud cover during the monsoon months (JJAS) leads to a reduction in insolation in the daytime (Kattel et al., 2012) and entrapment of upward longwave radiation during the nighttime (Bhutiyani et al., 2007), resulting in higher night surface temperatures. The difference in TLR in winter and summer can also be witnessed because of high natural convection in summer and owing to a temperature inversion in winter. These concomitant characteristics might contribute to the bimodal pattern TLR over the studied eastern Himalayan transect.

Conclusion

Mountains exert a significant influence on the normal meteorological characteristics of a region and have strong regulatory effects on the normal temperature regime. Moreover, the presence of forests on the mountain slope provides consistency to the variability of temperature across its altitudinal transect and leads to different temperature patterns above and below the treeline. This variation gets more pronounced on a seasonal basis and the range of drop in temperature is accentuated due to lack of vegetation above the tree line. The findings of this study indicate that the differing thermal behaviour above and below treeline environments in mountainous regions should be kept in mind, especially while studying the temperature-dependent geomorphological features like snow and glaciers in the Himalayas.

Application of uniform lapse rate across the altitudinal transect could be erroneous in the glacier mass balance or snowmelt runoff models. Also, the application of environmental lapse rate (i.e., 0.65°C/100 m) on the temperature data collected from low altitude overestimates the drop in temperature with altitude. Moreover, it provides uniformity to temperature trends at the higher altitude and the bimodal behaviour as observed in this study gets subdued. We expect that monthly and seasonal lapse rates presented in this study could be applied to non-monitored mountain valleys in the southern slopes of the eastern Himalayas and will improve the certainty of glacier/snowmelt modelling for the region. The results of this study could further be improved with more closely spaced weather stations and establishing lapse rates for other valleys in the eastern Himalayas could provide a better average value for its application in the glacier melt modelling of the region.

Acknowledgement

The authors are grateful to the Glacier Research Programme of The Energy and Resources Institute, New Delhi, for providing the necessary support to conduct field visits and use hydro-meteorological data from its Glacier Monitoring Observatory at East Rathong Glacier, Sikkim, India. The authors are also grateful to the International Centre for Integrated Mountain Development (ICIMOD) for providing scientific instruments as part of the HI-AWARE project's sub-component to TERI's Glacier Research Programme.

References

Agrawal, A. and Tayal, S., 2015. Mass balance reconstruction since 1963 and mass balance model for East Rathong Glacier, eastern Himalaya, using remote sensing methods. *Geografiska Annaler: Series A, Physical Geography*, **97(4):** 695-707. doi.org/10.1111/geoa.12109.

Azam, M.F., Wagnon, P., Vincent, C., Ramanathan, AL., Favier, V., Mandal, A. and Pottakkal, J.G., 2014. Processes governing the mass balance of Chhota Shigri Glacier (western Himalaya, India) assessed by point-scale surface energy balance measurements. *The Cryosphere*, **8(6):** 2195-2217.

Barnett, T.P., Adam, J.C. and Lettenmaier, D.P., 2005. Potential impacts of a warming climate on water availability in snow-dominated regions. *Nature*, **438(7066):** 303-309. doi:10.1038/nature04141.

Barry, R.G., Kiladis, G. and Bradley, R.S., 1981. Synoptic climatology of the Western United States in relation to climatic fluctuations during the twentieth century. *Journal of Climatology*, **1(2):** 97-113. doi: 10.1002/joc.3370010202.

Barry, R.G., 1992. Mountain Weather and Climate. 2nd ed. Routledge, London.

Bhutiyani, M.R., Kale, V.S. and Pawar, N.J., 2007. Long term trends in maximum, minimum and mean annual temperatures across the northwestern Himalaya during the twentieth century. *Climate Change*, **85:** 159-177. doi: 10.1007/s10584-006-9196-1

Blandford, T.R., Humes, K.S., Harshburger, B.J., Moore, B.C., Walden, V.P. and Ye, H., 2008. Seasonal and synoptic variations in near-surface air temperature lapse rates in a mountainous basin. *Journal of Applied*

Meteorology and Climatology, **47(1):** 249-261. doi: 10.1175/2007JAMC1565.1.

Bogren, J., Gustavsson, T. and Postgård, U., 2000. Local temperature differences in relation to weather parameters. *International Journal of Climatology*, **20(2):** 151-170, doi: 10.1002/(SICI)1097-0088(200002)20:2<151::AID-JOC460>3.0.CO;2-U.

Bolstad, P.V., Swift, L., Collins, F. and Régnière, J., 1998. Measured and predicted air temperatures at basin to regional scales in the southern Appalachian mountains. *Agricultural and Forest Meteorology*, **91(3-4):** 161-176, doi.org/10.1016/S0168-1923(98)00076-8

Chhetri, S.K., Singh, K.K. and Krishna, A.P., 2013. Resource use impacts within the forest land cover of Khangchendzonga Biosphere Reserve, Sikkim Himalaya along different disturbance levels and altitudinal zones. *Applied Ecology and Environmental Research*, **11(2):** 273-291.

Diaz, H.F. and Bradley, R.S., 1997. Temperature variations during the last century at high elevation sites. *In*: Climatic change at high elevation sites (pp. 21-47). Springer, Dordrecht.

Dodson, R. and Marks, D., 1997. Daily air temperature interpolated at high spatial resolution over a large mountainous region. *Climate Research*, **8(1):** 1-20. doi: 10.3354/cr008001.

Gardner, A.S., Sharp, M.J., Koerner, R.M., Labine, C., Boon, S., Marshall, S.J., Burgess, D.O. and Lewis, D., 2009. Near-surface temperature lapse rates over Arctic glaciers and their implications for temperature downscaling. *Journal of Clim*ate, **22(16):** 4281-4298, doi.org/10.1175/2009JCLI2845.1.

Hanna, E., Mernild, S.H., Yde, J.C. and Villiers, S.D., 2017. Surface air temperature fluctuations and lapse rates on Olivares Gamma Glacier, Rio Olivares basin, central Chile, from a novel meteorological sensor network. *Advances in Meteorology*, **2017(1):** 12-14, doi.org/10.1155/2017/6581537

Hansen, J., Ruedy, R., Sato, M. and Lo, K., 2010. Global surface temperature change. *Reviews of Geophysics*, **48(4)**.

Heynen, M., Miles, E., Ragettli, S., Buri, P., Immerzeel, W.W. and Pellicciotti, F., 2016. Air temperature variability in a high-elevation Himalayan catchment. *Annals of Glaciology*, **57(71):** 212-222. doi: 10.3189/2016AoG71A076.

Hock, R., 2003. Temperature index melt modelling in mountain areas. *Journal of Hydrology*, **282(1-4):** 104-115.

Immerzeel, W.W., Van Beek, L.P.H. and Bierkens, M.F.P., 2010. Climate change will affect the Asian water towers. Science, **328:** 1382-1385. doi:10.1126/ science.1183188.

Immerzeel, W.W., Petersen, L., Ragettli, S. and Pellicciotti, F., 2014. The importance of observed gradients of air temperature and precipitation for modeling runoff from a glacierized watershed in the Nepalese Himalayas. *Water Resources Research*, **50(3):** 2212-2226, doi.org/10.1002/2013WR014506.

IPCC, 2013. Climate Change 2013: The Physical Science Basis. Contribution of Working Group I to the Fifth Assessment Report of the Intergovernmental Panel on Climate Change. Stocker, T.F., Qin, D., Plattner, G.K., Tignor, M., Allen, S.K., Boschung, J., Nauels, A., Xia, Y., Bex, V. and Midgley, P.M. (eds). Cambridge University Press. Cambridge, United Kingdom and New York, USA.

Jones, P.D., 1994. Hemispheric surface air temperature variations: A reanalysis and an update to 1993. *Journal of Climate*, **7(11):** 1794-1802.

Joshi, R., Sambhav, K. and Singh, S.P., 2018. Near surface temperature lapse rate for treeline environment in western Himalaya and possible impacts on ecotone vegetation. *Tropical Ecology*, **59(2):** 197-209.

Kattel, D.B., Yao, T., Yang, K., Tian, L., Yang, G. and Joswiak, D., 2013. Temperature lapse rate in complex mountain terrain on the southern slope of the central Himalayas. *Theoretical and Applied Climatology*, **113(3):** 671-682. doi: 10.1007/s00704-012-0816-6.

Kattel, D.B., Yao, T., Yang, W., Gao, Y. and Tian, L., 2015. Comparison of temperature lapse rates from the northern to the southern slopes of the Himalayas. *International Journal of Climatology*, **35(15):** 4431-4443. doi: 10.1002/joc.4297.

Kattel, D.B., Yao, T., Ullah, K. and Rana, A.S., 2019. Seasonal near-surface air temperature dependence on elevation and geographical coordinates for Pakistan. *Theoretical and Applied Climatology*, 1-23.

Kattel, D.B. and Yao, T., 2013. Recent temperature trends at mountain stations on the southern slope of the central Himalayas. *Journal of Earth System Science*, **122(1):** 215-227.

Kattel, D.B. and Yao, T., 2018. Temperature–topographic elevation relationship for high mountain terrain: An example from the southeastern Tibetan Plateau. *International Journal of Climatology*, **38:** e901-e920, doi: 10.1002/joc.5418.

Kattel, D.B., Yao, T. and Panday, P.K., 2018. Near-surface air temperature lapse rate in a humid mountainous terrain on the southern slopes of the eastern Himalayas. *Theoretical and Applied Climatology*, **132(3):** 1129-1141. doi: 10.1007/s00704-017-2153-2.

Lundquist, J.D., Pepin, N. and Rochford, C., 2008. Automated algorithm for mapping regions of cold-air pooling in complex terrain. Journal of Geophysical Research: Atmospheres, 113(D22). doi.org/10.1029/2008JD009879.

Marshall, S.J., Sharp, M.J., Burgess, D.O. and Anslow, F.S., 2007. Near-surface-temperature lapse rates on the Prince of Wales Icefield, Ellesmere Island, Canada: Implications for regional downscaling of temperature. *International Journal of Climatology: A Journal of the Royal Meteorological Society*, **27(3):** 385-398. doi.org/10.1002/joc.1396.

Marshall, S.J. and Sharp, M.J., 2009. Temperature and melt modeling on the Prince of Wales ice field, Canadian

High Arctic. *Journal of Climate*, **22(6):** 1454-1468, doi:10.1175/2008JCLI2560.1.

Micu, D.M., Dumitrescu, A., Cheval, S. and Birsan, M.V., 2015. Projections of future changes in climate of the Romanian Carpathians. *In*: Climate of the Romanian Carpathians (pp. 199-205). Springer, Cham. doi: 10.1007/978-3-319-02886-6.

Pepin, N.C. and Lundquist, J.D., 2008. Temperature trends at high elevations: patterns across the globe. *Geophysical Research Letters*, **35(14):** 1-6. doi: 10.1029/2008GL034026.

Rangwala, I. and Miller, J.R., 2012. Climate change in mountains: A review of elevation-dependent warming and its possible causes. *Climatic Change*, **114(3):** 527-547. doi:10.1007/s10584-012-0419-3

Rolland, C., 2003. Spatial and seasonal variations of air temperature lapse rates in Alpine regions. *Journal of Climate*, **16(7):** 1032-1046.

Romshoo, S.A., Rafiq, M. and Rashid, I., 2018. Spatio-temporal variation of land surface temperature and temperature lapse rate over mountainous Kashmir Himalaya. *Journal of Mountain Science*, **15(3):** 563-576. doi: 10.1007/s11629-017-4566-x.

Singh, S., Bhardwaj, A., Singh, A., Sam, L., Shekhar, M., Martín-Torres, F.J. and Zorzano, M.P., 2019. Quantifying the congruence between air and land surface temperatures for various climatic and elevation zones of Western Himalaya. *Remote Sensing*, **11(24):** 2889.

Singh, V. and Goyal, M.K., 2016. Analysis and trends of precipitation lapse rate and extreme indices over North Sikkim eastern Himalayas under CMIP5ESM-2M RCPs experiments. *Atmospheric Research*, **167:** 34-60. doi: 10.1016/j.atmosres.2015.07.005.

Thayyen, R.J. and Dimri, A.P., 2014. Factors controlling slope environmental lapse rate (SELR) of temperature in the monsoon and cold-arid glacio-hydrological regimes of the Himalaya. *The Cryosphere Discussions*, **8(6):** 5645-5686. doi: 10.5194/tcd-8-5645-2014.

Thayyen, R.J. and Dimri, A.P., 2018. Slope environmental lapse rate (SELR) of temperature in the monsoon regime of the western Himalaya. *Frontiers in Environmental Science*, **6:** 1-20. doi: 10.3389/fenvs.2018.00042.

Thyer, N., 1985. Looking at western Nepal's climate. *Bulletin of the American Meteorological Society*, **66(6):** 645-650. doi: 10.1175/1520-0477(1985)066<0645:LAWNC>2.0.CO;2.

Yadav, J.S., Pratap, B., Gupta, A.K., Dobhal, D.P., Yadav, R.B.S. and Tiwari, S.K., 2019. Spatio-temporal variability of near-surface air temperature in the Dokriani glacier catchment (DGC), central Himalaya. *Theoretical and Applied Climatology*, **136(3):** 1513-1532. doi: 10.1007/s00704-018-2544-z.